

# Minimal model of financial stylized facts

Giacomo Bormetti

Scuola Normale Superiore, Pisa & INFN, Pavia

**joint work with**

Danilo Delpini

Dipartimento di Economia Politica e Metodi Quantitativi, Pavia

INFN, Pavia & CeRS - IUSS, Pavia

## Overview

- A mini-review of physical phenomena exhibiting non Gaussian features: from turbulent velocity flows to scaling Markov processes
- The Langevin equation with non linear diffusion
- Modeling the volatility
- Analytical results concerning stilyzed facts
- Conclusions and perspectives

# Markov properties of small-scale turbulence

R. Friedrich and J. Peinke, *Phys. Rev. Lett.* 78 (1997) p. 863-866

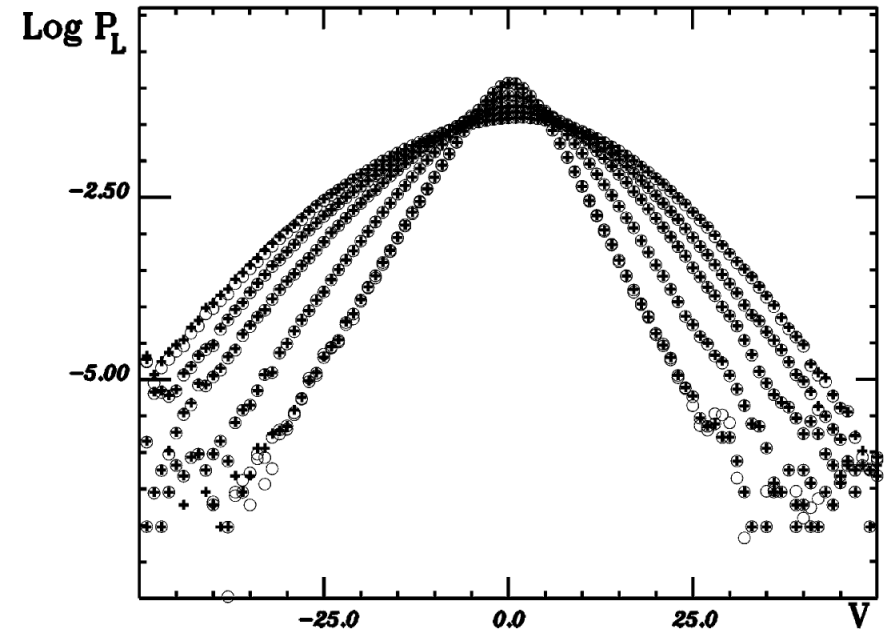
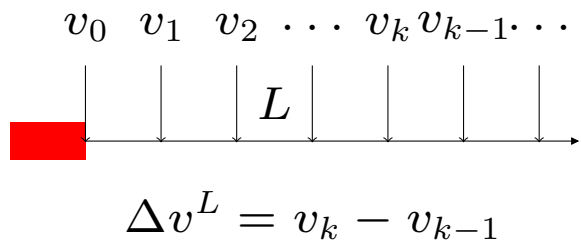
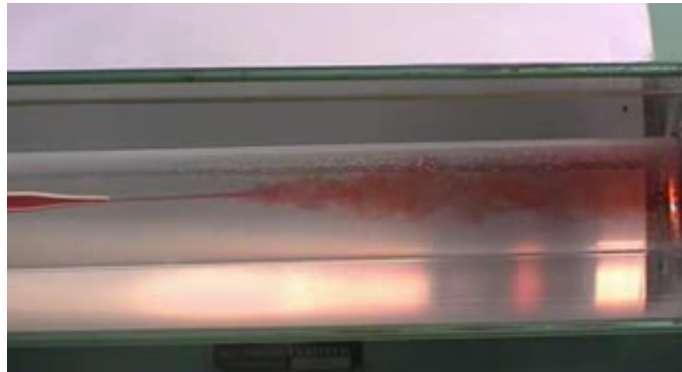


**Figure 1:** Probability density functions  $P_{L_i}(\Delta v_i)$  for  $L_i = 24, 54, 124, 224, 424$ .

## Markov properties in high frequency FX data

C. Renner, J. Peinke and R. Friedrich, *Physica A* 298 (2001) p. 499-520

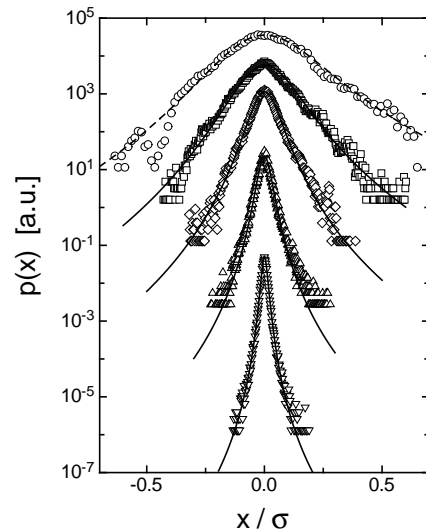


**Figure 2:** Comparison of the numerical solutions of the Fokker-Planck equation (solid lines) with the pdfs obtained directly from the data (open symbols). The scales  $\tau$  are (from top to bottom):  $\tau = 12\text{h}$ ,  $4\text{h}$ ,  $1\text{h}$ ,  $15\text{min}$  and  $4\text{min}$ .

The probability density  $p(x, \tau)$  obeys the Fokker-Planck equation

$$-\tau \frac{\partial p}{\partial \tau} = -\frac{\partial}{\partial x} (D_1(x, \tau)p) + \frac{\partial^2}{\partial x^2} (D_2(x, \tau)p) ,$$

while the stochastic process is generated by the Langevin equation (under Itô prescription)

$$-dx(\tau) = D_1(x, \tau)d\tau + \sqrt{\tau D_2(x, \tau)}dW(\tau) .$$

For the time series under consideration we have  $D_1(x, \tau) = -\gamma x$ ,  $\gamma = 0.93 \pm 0.02$  and  $D_2(x, \tau) = \alpha\tau + \beta x^2$ , with  $\alpha = 0.016 \pm 0.002$  and  $\beta = 0.11 \pm 0.02$ .

See also R. Friedrich, J. Peinke and Ch. Renner, *Phys. Rev. Lett.* 84 (2000) p. 5224 for more results.

## Power law spectra in $e^+e^-$ , $p\bar{p}$ and heavy ions collisions

G. Wilk and Z. Włodarczyk, *Phys. Rev. Lett.* 84 (2000) p. 2770

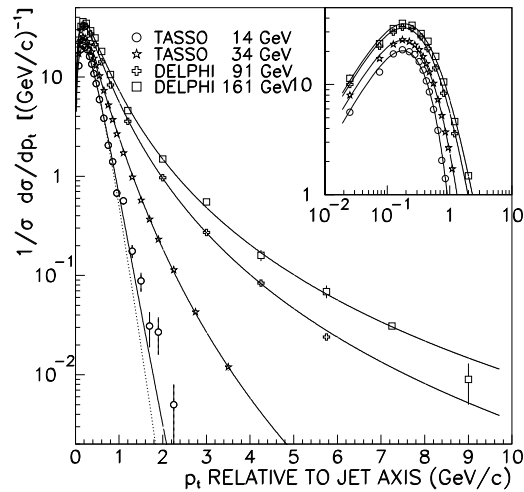


**Figure 3:** The distribution of the transverse momentum of charged hadrons with respect to jet axis is sketched for four different experiments, whose center of mass energies vary from 14 and 34 Gev (TASSO) up to 91 and 161 Gev (DELPHI).

See I. Bediaga, E. M. F. Curado and J. M. de Miranda, *Physica A* 286 (2000) p. 156-163.

Deviations from the Boltzmann-Gibbs exponential formula (dotted line) in favour of a Lévy like distribution are explained in terms of a Normal - Inverse Gamma mixture model.

The microscopic equation governing the temperature reads

$$dT(t) = \left( \phi - 2\frac{T}{\tau} + DT \right) dt + \sqrt{2DT^2} dW(t),$$

with  $\phi$ ,  $\tau$  and  $D$  all positive.

At the stationary state  $T \sim IG\left(\frac{1}{\tau D}, \frac{\phi}{D}\right)$ .

## Scaling and Markov processes

J. L. McCauley, G. H. Gunaratne and K. E. Bassler, *Physica A* 379 (2007) p. 1-9

- **Scaling**

$X_t = t^H X_1$ , where equality holds in distribution.

It is readily proved that  $\langle X_t^n \rangle = c_n t^{nH}$  and  $p(x, t) = t^{-H} F(x/t^H)$ .

- **A Markov process generated locally by a driftless SDE**

$$dX = \sqrt{D(X, t)} dW(t)$$

- Scaling implies  $D(X, t) = t^{2H-1} D(X/t^H)$
- Assume  $D(X/t^H) = D_0(1 + \epsilon X^2/t^{2H})$
- If  $H = 1/(3 - q)$  we obtain the process described in L. Borland, *Phys. Rev. Lett* 89 (2002) 098701.

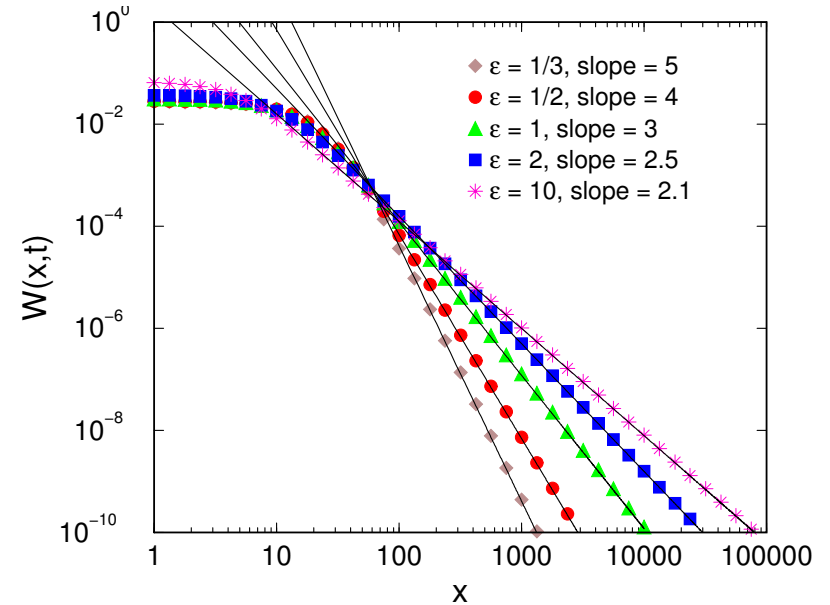


**Figure 4:** Log-log plot of the distribution of  $X_t$  using a quadratic diffusion coefficient showing the emergence of power-law tails.

See A. L. Alejandro-Quiñones *et al.*, *Physica A* 363 (2006) p. 383-392.

## The microscopic equation

G. Borretti and D. Delpini, *Phys. Rev. E* 81 (2010) p. 032102

$$dX_t = \frac{aX_t + b}{g(t)} dt + \sqrt{\frac{cX_t^2 + dX_t + e}{g(t)}} dW_t ,$$

with initial time condition  $X_{t_0} = X_0$ ,  $t_0 \in D \subseteq [0, t_{\text{lim}})$  with  $t_{\text{lim}}$  possibly  $+\infty$ ;  $W_t$  is the standard Brownian motion,  $a$ ,  $b$ ,  $c$ ,  $d$ , and  $e$  are real constants,  $1/g(t)$  is a non negative smooth function of the time over  $D$ .

Application of the Itô Lemma to  $f(X_t) = X_t^n$  leads to relation

$$\begin{aligned} X_t^n = & X_0^n + \int_{t_0}^t \frac{X_s^{n-2}}{g(s)} \left[ F_n X_s^2 + A_n X_s + B_n \right] ds \\ & + n \int_{t_0}^t \frac{X_s^{n-1}}{\sqrt{g(s)}} \sqrt{cX_s^2 + dX_s + e} dW_s , \end{aligned}$$

where the coefficients read  $F_n = na + \frac{1}{2}n(n-1)c$ ,  $A_n = nb + \frac{1}{2}n(n-1)d$ ,  $B_n = \frac{1}{2}n(n-1)e$ .

## Moments recursive relation

Expectation of the previous Equation provides the linear ordinary differential equation (ODE) satisfied by the  $n$ -th order moment  $\mu_n(t) = \langle X_t^n \rangle$

$$g(t) \frac{d}{dt} \mu_n(t) = F_n \mu_n(t) + A_n \mu_{n-1}(t) + B_n \mu_{n-2}(t) .$$

In terms of the monotonously increasing function  $\tau(t) = \int_{t_0}^t 1/g(s) ds$ , the solution reads

$$\mu_n(t) e^{-F_n \tau(t)} = \langle X_0^n \rangle + A_n \int_0^{\tau(t)} \tilde{\mu}_{n-1}(s) e^{-F_n s} ds + B_n \int_0^{\tau(t)} \tilde{\mu}_{n-2}(s) e^{-F_n s} ds .$$

The previous expression lends itself to an expansion over  $\langle X_0^{n-j} \rangle$ , for  $j = 0, \dots, n$  by iteratively substituting the moments entering the r.h.s. with their closed-form solutions starting from  $\mu_0(t) = 1$ .



## Algorithmic solution

We define type  $A$  and type  $B$  “knots” of order  $k$  whose contributions are

$$\overset{\mathbb{A}_k}{\circ} = A_k \int_0^\tau e^{a_k \tau'} d\tau' \quad \text{and} \quad \overset{\mathbb{B}_k}{\bullet} = B_k \int_0^\tau e^{b_k \tau'} d\tau',$$

with  $a_k = -(F_k - F_{k-1})$  and  $b_k = -(F_k - F_{k-2})$ . We now consider ordered sequences of knots obtained applying the following rules:

- fix the order of the moment  $n \in \{1, \dots, N\}$ ;
- fix  $j \in \{1, \dots, n\}$ ;
- choose the first knot between  $\overset{\mathbb{A}_n}{\circ}$  or  $\overset{\mathbb{B}_n}{\bullet}$ ;
- move rightward adding a new knot:  $\overset{\mathbb{A}_k}{\circ}$  can be followed by either  $\overset{\mathbb{A}_{k-1}}{\circ}$  or by  $\overset{\mathbb{B}_{k-1}}{\bullet}$ , while  $\overset{\mathbb{B}_k}{\bullet}$  can be followed by either  $\overset{\mathbb{A}_{k-2}}{\circ}$  or  $\overset{\mathbb{B}_{k-2}}{\bullet}$ ;
- if  $N_A$  and  $N_B$  are the number of type  $A$  and type  $B$  knots, respectively, stop when  $N_A + 2N_B = j$ .

## Example: $n = 4$

- $j = 0$  is associated to a sequence with no knot whose contribution is equal to 1.
- $j = 1$ : the only admissible sequence is  $\overset{\mathbb{A}_n}{\circ}$ .
- $j = 2$ : beside  $\overset{\mathbb{B}_n}{\bullet}$ , we have to consider the sequence  $\overset{\mathbb{A}_n}{\circ} \overset{\mathbb{A}_{n-1}}{\circ}$  giving the contribution

$$\overset{\mathbb{A}_n}{\circ} \overset{\mathbb{A}_{n-1}}{\circ} = A_n A_{n-1} \int_0^\tau e^{a_n \tau_1} \int_0^{\tau_1} e^{a_{n-1} \tau_2} d\tau_2 d\tau_1 .$$

- $j = 4$ : the following strings have to be taken into account

$$\begin{array}{ccc} \overset{\mathbb{A}_n}{\circ} \overset{\mathbb{A}_{n-1}}{\circ} \overset{\mathbb{A}_{n-2}}{\circ} \overset{\mathbb{A}_{n-3}}{\circ} & \overset{\mathbb{A}_n}{\circ} \overset{\mathbb{A}_{n-1}}{\circ} \overset{\mathbb{B}_{n-2}}{\bullet} & \\ \overset{\mathbb{A}_n}{\circ} \overset{\mathbb{B}_{n-1}}{\bullet} \overset{\mathbb{A}_{n-3}}{\circ} & \overset{\mathbb{B}_n}{\bullet} \overset{\mathbb{A}_{n-2}}{\circ} \overset{\mathbb{A}_{n-3}}{\circ} & \overset{\mathbb{B}_n}{\bullet} \overset{\mathbb{B}_{n-2}}{\bullet} . \end{array}$$

## Algorithmic solution

Once  $n$  has been fixed, it is readily proved that every sequence is univocally determined retaining the label of the vertex while dropping the indexes.

For the case  $j = 4$  previous strings reduce to  $\begin{array}{cccc} \text{A} & \text{A} & \text{A} & \text{A} \\ \circ & \circ & \circ & \circ \end{array}$   $\begin{array}{ccc} \text{A} & \text{A} & \text{B} \\ \circ & \circ & \bullet \end{array}$   $\begin{array}{ccc} \text{A} & \text{B} & \text{A} \\ \circ & \bullet & \circ \end{array}$   $\begin{array}{ccc} \text{B} & \text{A} & \text{A} \\ \bullet & \circ & \circ \end{array}$   $\begin{array}{cc} \text{B} & \text{B} \\ \bullet & \bullet \end{array}$ .

We now call  $\Pi_{N_A N_B}$  the set of permutations with no repetition of  $N_A$  type  $A$  elements and  $N_B$  type  $B$  elements and  $\pi_{N_A N_B}$  its generic element. The compact notation  $\Delta_n(\pi_{N_A N_B}, \tau(t))$  identifies the  $N_A + N_B$ -dimensional integral contributing to the  $n$ -th moment and corresponding to the sequence of knots sorted according to  $\pi_{N_A N_B}$ .

In terms of the above quantities, the expression of  $\mu_n(t)$  can be usefully rewritten in the compact form

$$\mu_n(t) = e^{F_n \tau(t)} \sum_{j=0}^n \langle X_0^{n-j} \rangle \sum_{N_A + 2N_B = j} \sum_{\Pi_{N_A N_B}} \Delta_n(\pi_{N_A N_B}, \tau(t)) .$$

## Algorithmic solution

A careful analysis of the quantity  $\Delta_n(\pi_{N_A N_B}, \tau(t))$  shows that it can always be computed analytically in an algorithmic way, which makes the expansion in the previous page a powerful tool to exactly compute  $\mu_n$  up to an arbitrary order. Supposing that all the  $a_k$  and  $b_k$  involved in the expression of  $\mu_n$  are non vanishing, it can be rewritten as

$$\mu_n(t) = \sum_{j=0}^n c_j^n e^{F_{n-j}\tau(t)},$$

the  $c_j^n$  being real possibly vanishing constants.

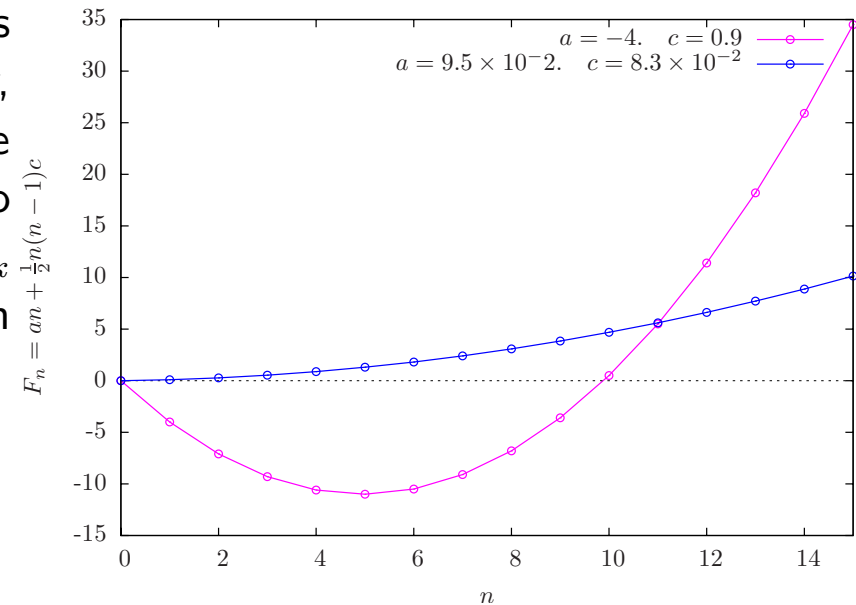


Figure 5: Behavior of  $F_n$  vs  $n$ .

## $g(t)$ affects the time scaling of the process

The Equation in previous slide provides evidence of the typical scaling of the moments over time. The multiple time scales emerging from the multiplicative noise process can be affected by varying the functional form of  $g(t)$ .

- For a constant  $g(t) = 1$ , we have  $\tau = t - t_0$  and the  $n$ -th order moment is characterized by the superposition of  $n$  exponentials with time constants  $\{1/|F_n|, \dots, 1/|F_1|\}$ .
- When  $g(t) = t$ , we have terms of the form

$$e^{F_{n-j}\tau(t)} = t^{F_{n-j}} t_0^{-F_{n-j}},$$

producing a power law time scaling of the moments.

- More generally, for  $g(t) = t^\beta$  ( $\beta \neq 1$ ) the time dependence turns out to be a stretched exponential with stretching exponent  $1 - \beta$ :

$$e^{F_{n-j}\tau(t)} = e^{F_{n-j} \frac{1}{1-\beta} (t^{1-\beta} - t_0^{1-\beta})}.$$

## Scaling: analytical vs Monte Carlo

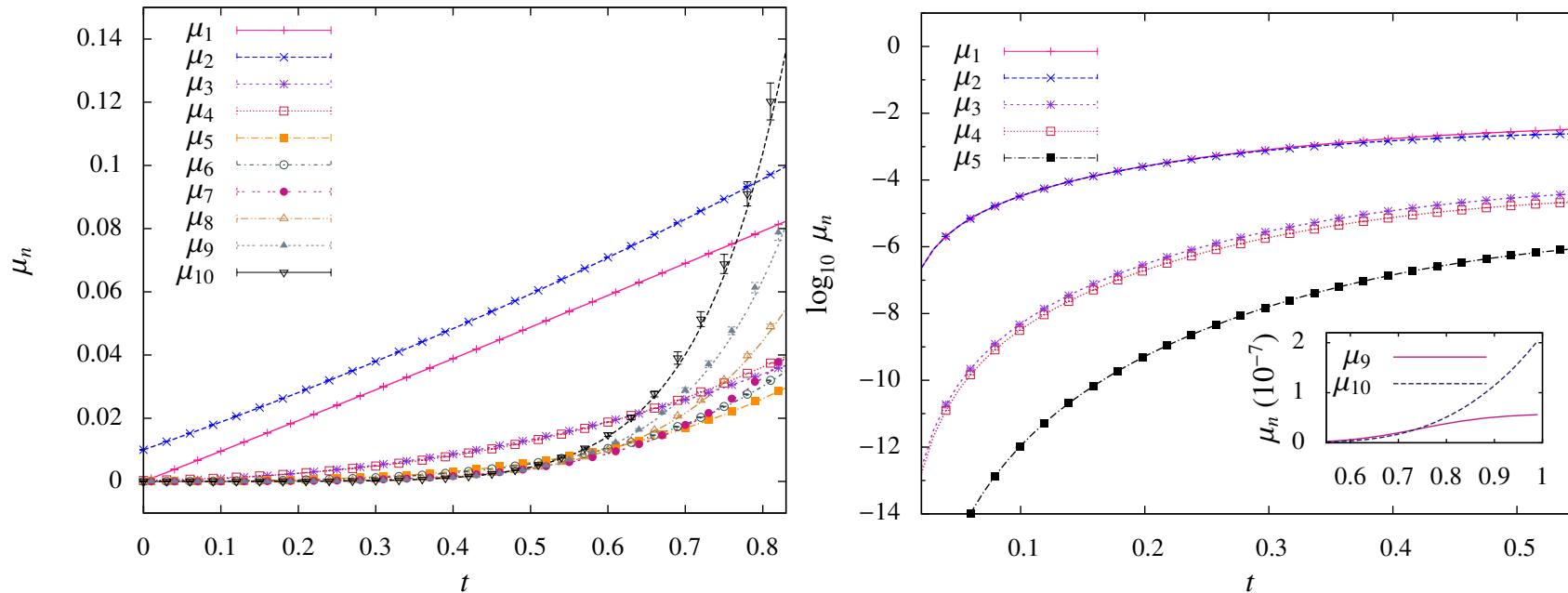


**Figure 6: (Left) Scaling of the moments for  $a = b = 9.5 \times 10^{-2}$  and  $c = d = e = 8.3 \times 10^{-2}$ . (Right) Lowest order moments for  $a = -20$ ,  $b = d = e = 0.1$ ,  $c = 4.5$ , with  $g = t^\beta$ ,  $\beta = 2$  and  $\tilde{p}_{t_0}(x) = \delta(x)$ . In the inset the last converging moment is compared to the first diverging one.**

## The stationary solution

As far as the PDF  $p(x, t)$  associated to above process is concerned, we can draw some conclusion when we have a diverging  $\tau$ . Indeed, in terms of  $\tau$  the PDF satisfies the FP equation

$$\frac{\partial}{\partial \tau} \tilde{p}(x, \tau) = -\frac{\partial}{\partial x} [D_1(x) \tilde{p}(x, \tau)] + \frac{1}{2} \frac{\partial^2}{\partial x^2} [D_2(x) \tilde{p}(x, \tau)] ,$$

with  $D_1(x) = ax + b$  and  $D_2(x) = cx^2 + dx + e$  and initial condition  $\tilde{p}(x, 0) = \tilde{p}_0(x)$ .

- The stationary solution reads

$$\tilde{p}_{\text{st}}(x) = \frac{N}{D_2(x)} \exp \left\{ \int_0^x dx' \frac{D_1(x')}{D_2(x')} \right\}$$

- The smoothness of  $\tau$  as a function of  $t$  implies

$$\lim_{t \rightarrow t_{\text{lim}}^-} p(x, t) = \lim_{\tau \rightarrow +\infty} \tilde{p}(x, \tau) = \tilde{p}_{\text{st}}(x)$$

## The asymptotic PDF

- **Case  $a = 0$  and  $e > 0$ .** If  $c = 0$ , then also  $d$  is 0 and the Langevin Equation (LE) describes an Arithmetic Brownian motion. If  $c > 0$ , no moment converge and the stationary solution is a power law with tail exponent  $\nu = 1$ .
- **Case  $a < 0$ ,  $c > 0$ , and  $e > 0$ .**  $F_n > 0$  for  $n > n_1 = 1 - 2a/c$ , thus only the first  $n < n_1$  moments converge to a stationary level. The solution of the FP equation predicts the emergence of power law tails with  $\nu = n_1$ .
- **Case  $a \neq 0$ ,  $c = 0$ , and  $e > 0$ .** The LE describes an Ornstein-Uhlenbeck process.
- **Case  $a < 0$ ,  $e = 0$  and  $c > 0$ .** The stationary solution is an Inverse Gamma with shape parameter  $n_1 > 0$  and scale parameter  $2|b|/c > 0$ . If  $b > 0$  the Inverse Gamma is defined for  $x \in [0, +\infty)$ , while for  $b < 0$  the support is  $(-\infty, 0]$ .



## Stochastic volatility and multiplicative noise diffusion

D. Delpini and G. Bormetti, Minimal model of financial stylized facts. *To appear on Phys. Rev. E*

Let's consider the following stochastic volatility model

$$\begin{cases} dX_t = \sigma_t dW_{1,t} , & \sigma_t = mY_t^\beta \\ dY_t = (aY_t + b)dt + \sqrt{cY_t^2 + dY_t + e} dW_{2,t} \end{cases}$$

where the two processes are correlated through  $\langle dW_{1,t} dW_{2,s} \rangle = \rho \delta(t - s) dt$ ,  $a < 0$ , and the price process  $S_t$  is related to  $X_t$  through the relation  $S_t = S_0 e^{\mu t + X_t}$ .

IS THIS DYNAMICS MEANINGFUL? **Yes, since it generalizes.**

- $d = e = 0$  and  $\beta = 1/2 \longrightarrow$  **Hull-White**
- $c = d = 0$  and  $\beta = 1 \longrightarrow$  **Stein-Stein**
- $c = e = 0$ ,  $d > 0$  + Feller condition and  $\beta = 1/2 \longrightarrow$  **Heston**

## The volatility distribution: empirical results

P. Cizeau, Y. Liu, M. Meyer, C.-K. Peng and H. E. Stanley, *Physica A* 245 (1997) p. 441-445

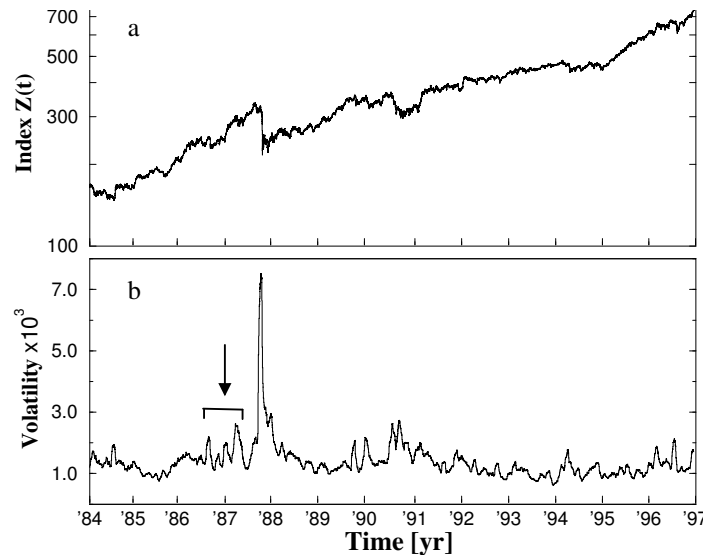


**Figure 7:** (Top) The S&P 500 index  $Z(t)$  for the 13-year period 1 Jan 1984 - 31 Dec 1996 at interval of 1 min. (Bottom) Volatility  $v_T(t)$  with  $T = 8190\text{min}$  and  $\Delta t = 30\text{min}$ .

$$v_T(t) = \frac{\Delta t}{T} \sum_{t'=t}^{t+T} \left| \frac{1}{A(t')} \log \frac{Z(t'+\Delta t)}{Z(t')} \right|$$

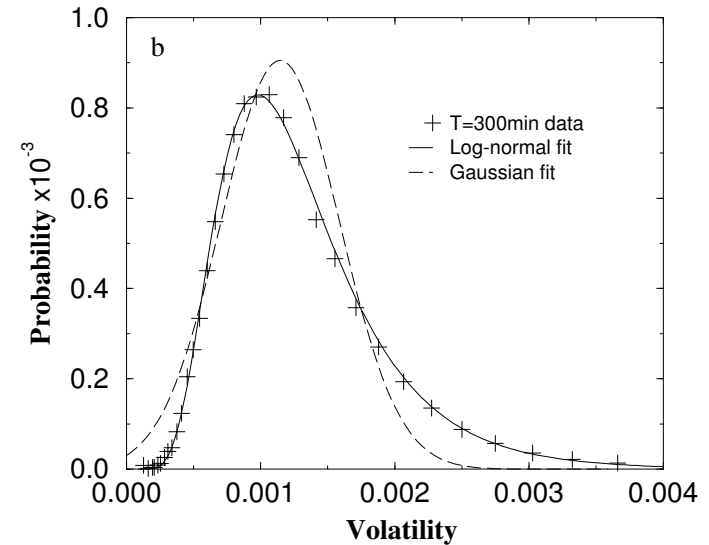


**Figure 8:** Comparison of the best log-normal and Gaussian fits for the 300min data.

## A realistic model should reproduce the volatility PDF

S. Miccichè, G. Bonanno, F. Lillo and R. N. Mantegna, *Physica A* 314 (2002) p. 756-761

The Inverse Gamma nature of the volatility emerges as the limit  $d, e \rightarrow 0$  (with  $a < 0, b, c > 0$ )

$$\begin{cases} dX_t = \sqrt{c} Y_t dW_t, & X_0 = 0 \\ dY_t = (aY_t + b)dt + \sqrt{c} Y_t dW_{2,t}, & Y_{t_0} = y_0 \end{cases}$$

$Y_t$  relaxes toward an Inverse Gamma distribution

$$p_{IG}(\sigma; \alpha, \beta) = \frac{\beta^\alpha}{\Gamma(\alpha)} \frac{e^{-\beta/\sigma}}{\sigma^{\alpha+1}}$$

with **shape**  $\alpha = 1 - \frac{2a}{c}$  and **scale**  $\beta = \frac{2b}{c}$ .

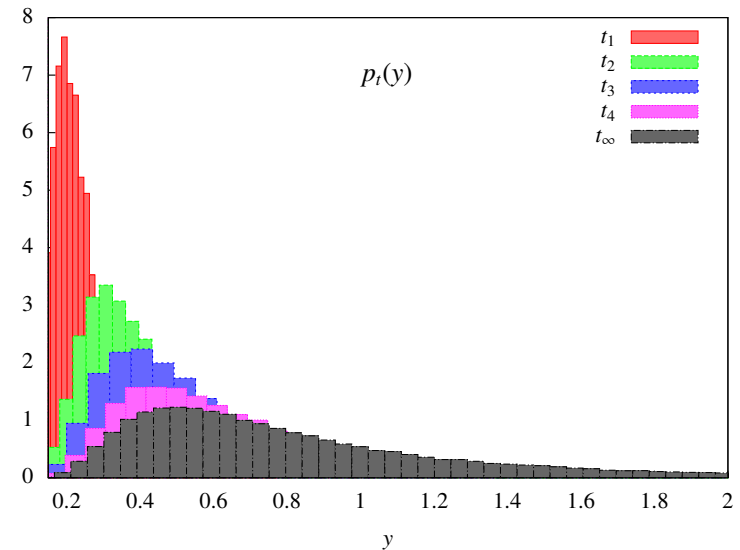


**Figure 9:** Dynamic evolution of  $Y_t$  with initial time condition  $\delta(Y - Y_0)$ ,  $Y_0 = 0$ . Parameters are fixed arbitrarily,  $\alpha = 3$  and  $\beta = 2$ ,  $a = -3$ .

## and predict the emergence of fat tails

H. E. Stanley and R. N. Mantegna, *Introduction to Econophysics: Correlations and Complexity in Finance* (1999).

A realistic model needs to reproduce the **excess of kurtosis** and the **skewed** nature of daily financial returns.

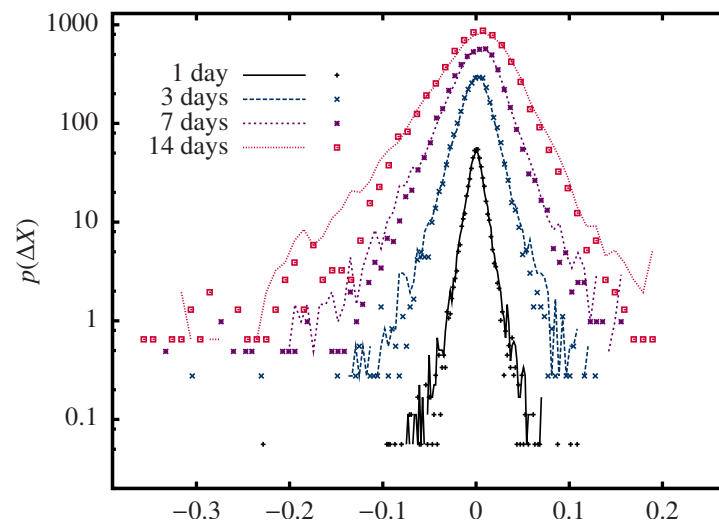


**Figure 10:** In log-linear scale, probability distributions for S&P500 returns (1970-2010), shifted for readability.

- Inheritance of scaling properties from the  $\mu_n$  through correlations

$$\langle X_t^n \rangle = \frac{1}{2} n(n-1)c \int_0^t ds \langle X_s^{n-2} Y_s^2 \rangle$$

- The simplest example:

$$\langle X_t^2 \rangle = c \int_0^t ds \mu_2^Y(s; t_0)$$

with

$$\mu_n^Y(t; t_0) = \sum_{j=0}^n c_j^n \exp[F_j(t - t_0)]$$

## Recursive structure of correlations

**Case study:** the third moment  $\langle X_t^3 \rangle = 3c \int_0^t ds \langle X_s Y_s^2 \rangle$

- Correlation  $\langle X_t Y_t^2 \rangle$  is linked to  $\langle X_t Y_t \rangle$  as solution of the ODE

$$\frac{d}{dt} \langle X_t Y_t^2 \rangle = F_2 \langle X_t Y_t^2 \rangle + A_2 \langle X_t Y_t \rangle + 2\rho c \mu_3^Y(t; t_0)$$

- . . . but a similar ODE is satisfied by  $\langle X_t Y_t \rangle$ :  $\frac{d}{dt} \langle X_t Y_t \rangle = F_1 \langle X_t Y_t \rangle + \rho c \mu_2^Y(t; t_0)$
- So, the solution for  $\langle X_t Y_t \rangle$  is known

$$\langle X_t Y_t \rangle = e^{at} \langle X_0 Y_0 \rangle + \rho c \int_0^t e^{as} \mu_2^Y(s; t_0) ds$$

. . . and recursively we can solve for  $\langle X_t Y_t^2 \rangle$ .

**Take home message:**  $\langle X^n \rangle$  diverges whenever the  $\mu_n^Y(t; -\infty)$  does.

## Digression about Novikov theorem

E. A. Novikov, *Soviet Physics JETP* 20, 1290 (1965).

Suppose you have a well defined functional  $f(t; [\xi])$ , depending on the  $n$ -dimensional Gaussian white noise  $\xi = (\xi_1, \xi_2, \dots, \xi_n)$ . The Novikov theorem allows to compute Wiener expectations in the form

$$\langle f(t; [\xi]) \xi_j(t') \rangle = \left\langle \frac{\delta f(t; [\xi])}{\delta \xi_j(t')} \right\rangle$$

where, in general, the components  $\xi_j(t)$  have a definite correlation structure:

$$\langle \xi_i(s) \xi_j(t) \rangle = \rho_{ij} \delta(t - s) \quad \Rightarrow \quad \frac{\delta}{\delta \xi_j} = \rho_{ij} \frac{\delta}{\delta \xi_i}$$

Heuristic approach:

$$\langle f(t; [\xi]) \xi(t') \rangle = \int f(t; [\xi]) \xi(t') \frac{1}{\sqrt{2\pi}} e^{-\frac{\xi(t')^2}{2}} d\xi(t') = \left[ -f(t; [\xi]) \frac{1}{\sqrt{2\pi}} e^{-\frac{\xi(t')^2}{2}} \right]_{\partial} + \int \frac{\delta f(t; [\xi])}{\delta \xi(t')} \frac{1}{\sqrt{2\pi}} e^{-\frac{\xi(t')^2}{2}} d\xi(t')$$

## Digression about a useful functional derivative

J. Perello and J. Masoliver, *Phys. Rev. E* 67 (2003).

We are working with mean-reverting processes for  $Y_t$  of the form (naively)

$$\dot{Y}_t = \alpha(\theta - Y_t) + D(Y_t)\xi(t)$$

whose stationary solution can be cast in the form

$$Y_t = \theta + \int_{-\infty}^t e^{-\alpha(t-t')} D(Y_{t'})\xi(t')dt' .$$

The following result reminiscent of the **Dyson expansion** holds, and it is a powerful tool in computing correlation functions

$$\frac{\delta Y_{t+\tau}}{\delta \xi(t)} = H(\tau)e^{-\alpha\tau} D(Y_t) e^{\int_t^{t+\tau} D'(Y_s)\xi(s)ds}$$

where  $D'$  stands for the derivative of  $D(Y)$  with respect to the process  $Y_t$ .

## Leverage correlation

Estimate of the correlation between past returns and future volatility ( $|a|/c > 1$ )

$$\mathcal{L} = \frac{\langle dX_{t+\tau}^2 dX_t \rangle}{\langle dX_t^2 \rangle^2} = \frac{\langle Y_{t+\tau}^2 Y_t \xi_1(t) \rangle}{\mu_2^Y(t; t_0)^2} \stackrel{t_0 \rightarrow -\infty}{=} -\rho H(\tau) \frac{a(2a+c)}{b(a+c)} \exp\left(-\frac{2|a|-c}{2}\tau\right)$$

### Sketch of the proof

- Application of the Novikov theorem gives

$$\langle Y_{t+\tau}^2 Y_t \xi_1(t) \rangle = 2\rho \left\langle Y_{t+\tau} Y_t \frac{\delta Y_{t+\tau}}{\delta \xi_2(t)} \right\rangle = 2c\rho e^{a\tau} H(\tau) \left\langle Y_t^2 Y_{t+\tau} e^{\sqrt{c} \int_t^{t+\tau} dW_{2,s}} \right\rangle$$

- Somewhat messy calculations prove that the function  $f(Y; t, \tau) \doteq \left\langle Y_t^2 Y_{t+\tau} e^{\sqrt{c} \int_t^{t+\tau} dW_{2,s}} \right\rangle$  is solution of an **integral Volterra equation**

$$f(Y; t, \tau) - (a+c) \int_0^\tau f(Y; t, \tau') e^{\frac{c}{2}(\tau-\tau')} d\tau' = e^{\frac{c}{2}\tau} \left[ \mu_3^Y(t; t_0) + b\tau \mu_2^Y(t; t_0) \right].$$



## To fix the parameter focus on stylized facts

Define  $A = \frac{\langle |\Delta X| \rangle}{\langle |\Delta W_1| \rangle} = -\frac{b\sqrt{c}}{a}$ ,  $B = \frac{\langle \Delta X^2 \rangle}{\Delta t} = \frac{2b^2c}{(2a+c)a}$ , and compute  $\frac{B}{2(B-A^2)} = -\frac{a}{c}$ .

Compute  $\frac{\langle |\Delta X|^3 \rangle}{\langle |\Delta W_1|^3 \rangle} = -\frac{2b^3c^{3/2}}{(a+c)(2a+c)a}$ . Fit  $\tau^{\mathcal{L}} = \frac{2}{2|a|-c}$ . Estimate  $\mathcal{L}(0^+) = -\rho \frac{a(2a+c)}{b(a+c)}$ .

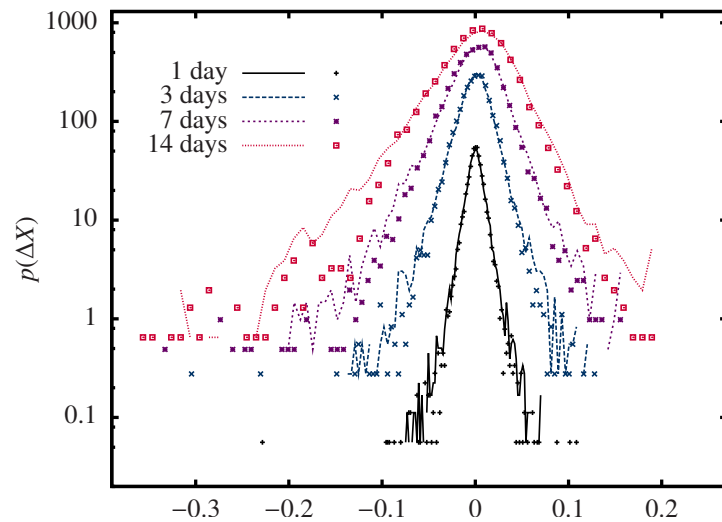


**Figure 11:** In log-linear scale, probability distributions for S&P500 returns (1970-2010), shifted for readability.

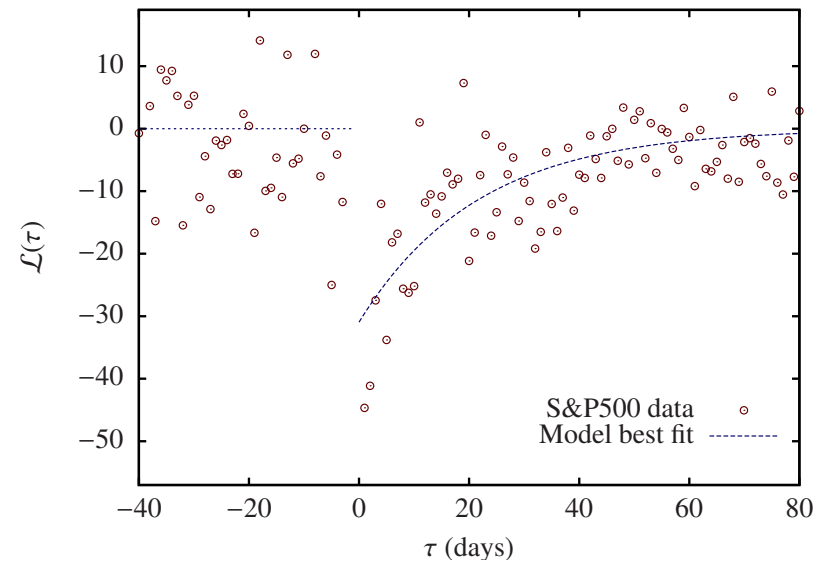


**Figure 12:** Best fit of the empirical leverage correlation for S&P500 returns (1970-2010).

## Volatility autocorrelation

Parameter	Estimate from S&P500	
$a$	-16.0608	yr <sup>-1</sup>
$b$	0.8627	yr <sup>-1</sup>
$c$	8.9749	yr <sup>-1</sup>
$\rho$	-0.5089	

**Table 1: Model parameters estimated from the daily log-returns of the S&P500 index during 1970-2010.**

$$\frac{|a|}{c} > \frac{3}{2}$$

the moments of  $Y_t$  up to the order  $n = 4$  do converge asymptotically.

$$\mathcal{A}(\tau; t) = \frac{\langle dX_t^2 dX_{t+\tau}^2 \rangle - \langle dX_t^2 \rangle \langle dX_{t+\tau}^2 \rangle}{\sqrt{\text{VaR}[dX_t^2]} \sqrt{\text{VaR}[dX_{t+\tau}^2]}}$$

The Novikov theorem allows to deal with  $\langle dX_t^2 dX_{t+\tau}^2 \rangle$ , and the stationary limit to approximate  $\text{Var}[dX_{t+\tau}^2] \approx \text{Var}[dX_t^2] = c^2 \left[ 3\mu_4^Y(t; -\infty) - \mu_2^Y(t; -\infty)^2 \right] dt^2$ .

The final result reads

$$\mathcal{A}(\tau) = \frac{1}{D} \left[ N_1 e^{-|a|\tau} + N_2 e^{-2\tau/\tau_{\mathcal{L}}} \right],$$

with coefficients

$$D = \frac{1}{c^2} \left( 4a^2 - 2ac - 3c^2 \right) (a + c)$$

$$N_1 = -\frac{1}{c} (2a + 3c) (2a + c), \quad N_2 = a.$$

## Volatility autocorrelation

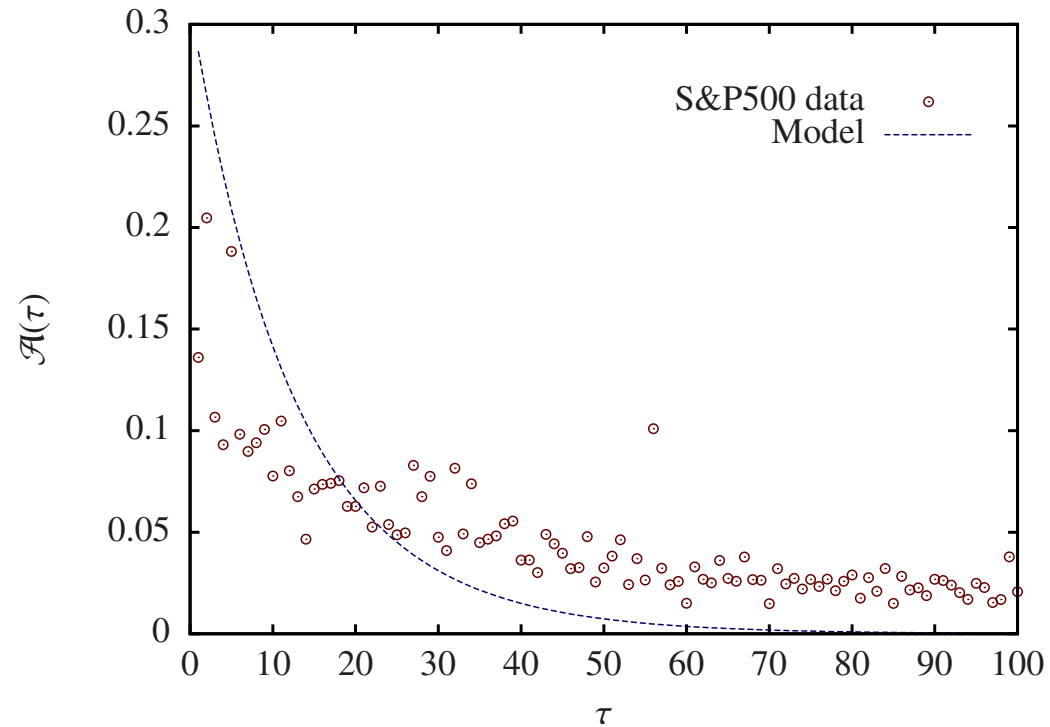


**Figure 13:** Theoretical prediction for the volatility autocorrelation function of the daily returns of the S&P500 index 1970-2010.  $\tau^{\mathcal{L}}/2 \sim 10$  days,  $-1/a \sim 15$  days, and  $\tau^{\mathcal{L}} \sim 20$  days.

## Conclusions and perspectives

- Multiplicative noise diffusion process (MNDP): from turbulence to finance.
- Rich scaling properties, analytically characterized at the level of the moments.
- MNDP as a natural candidate to describe the dynamics of the volatility.
- Minimal stochastic volatility model ( $d, e = 0$ ) correctly predicts
  - **Inverse Gamma distribution of  $\sigma$**
  - **power-law tails for  $X$**
  - **aggregated Gaussianity**
  - **zero returns autocorrelation**
  - **exponential scaling for the leverage**
  - **non trivial scaling of volatility autocorrelation**
- we are currently working on a simple extension to capture the persistence of volatility